Downloaded from http://polymerphysics.net

ELSEVIER

Journal of Non-Crystalline Solids 182 (1995) 172–179

JOURNAL OF NON-CRYSTALLINE SOLIDS

An interpretation of quasielastic neutron scattering and molecular dynamics simulation results on the glass transition

K.L. Ngai [a,*], C.M. Roland [a], G.N. Greaves [b]

[a] *Naval Research Laboratory, Code 6800, 4555 Overlook Ave., Washington, DC 20375-5320, USA*
[b] *EPSRC Daresbury Laboratory, Warrington, WA4 4AD, UK*

Abstract

Results of recent molecular dynamics simulations and quasielastic neutron scattering experiments performed on several glass-forming materials are discussed and analyzed to show that they are in agreement with the fundamental laws of relaxation proposed by the coupling model. Specifically, these results exhibit the existence of a temperature independent time, at which the correlation function crosses over from an exponential form, $\exp-(t/\tau_0)$, which holds for $t < t_c$ to a stretched exponential correlation function, $\exp-(t/\tau^*)^{1-n}$, which holds for $t > t_c$. Continuity of the correlation function at $t = t_c$ leads to the important relation: $\tau^* = [t_c^{-n}\tau_0]^{1/(1-n)}$ which has been formerly applied to explain many aspects of the dynamics of glass-forming materials. The characteristics of τ_0 indicate that it is the relaxation time of an independently relaxing species in accordance with the model.

1. Introduction

The glass transition is one of the oldest problems in physical science that has still not been resolved. One can date the first study of the glass transition to prehistoric times, when Babylonians and Egyptians made glass from desert sand. Over the course of time many different kinds of glass-forming materials have been found. Today we have glasses formed from inorganic, organic, metallic and polymeric materials. The study of the dynamics of glass-forming liquids and the search for a basic understanding of the glass transition phenomenon have not abated. In fact recently there is renewed interest from the physics community in this problem, as evidenced by the applications of microscopic probe experiments including quasielastic neutron scattering [1–6] and molecular dynamics simulations [7–9]. We have also witnessed a surge in theoretical efforts to interpret these experiments [10–12]. Quasielastic neutron scattering (QENS) experiments and molecular dynamics simulations (MDS) can both monitor the dynamics of glass-forming liquids in the short time regime defined (approximately $10^{-14} < t < 10^{-9}$ s). This ability is to be contrasted with the much longer timescale (typically 10^2 s) associated with the conventional glass transition temperature, T_g. In spite of this disparity in timescales, QENS and MDS are crucial as microscopic probes that can critically test any microscopic theory or model of the glass transition.

QENS and MDS data have been published in the literature. The principal experimental results for diffusive motion of the atoms are contained in (i) the van Hove self-correlation function defined by $G_s(r, t) = \langle \delta[\{r_i(t) - r_i(0)\} - r]\rangle$, or (ii) equiva-

* Corresponding author. Tel: +1-202 767 6150. Telefax: +1-202 767 0546. E-mail: ngai@estd.nrl.navy.mil.

0022-3093/95/$09.50 © 1995 Elsevier Science B.V. All rights reserved

lently the intermediate scattering function defined by $F_s(Q, t) = \langle \exp\{-iQ[r_i(t) - r_i(0)]\}\rangle$, which is the spatial Fourier transform of $G_s(r, t)$, or (iii) the dynamic structure factor, $S_s(Q, \omega)$, given by the temporal Fourier transform of $F_s(Q, t)$ or (iv) the susceptibility, $\chi''(Q, \omega)$, which is the product $\omega S_s(Q, \omega)$. Experimental data represented by any of these functions contain contributions not only from the diffusive motion of the atoms but also from their vibrations (i.e., phonons). Thus, in comparing experiment with theory, it is of paramount importance to take into account the contribution of phonons to the relaxation data. There is evidence that relaxational and vibrational scattering are statistically independent processes, which justifies writing the intermediate scattering function as a product $F_s(Q, t) = F_{relax}(Q, t)F_{phonon}(Q, t)$ and the dynamic structure factor as a convolution $S_s(Q, \omega) = S_{relax}(Q, \omega) \otimes S_{phonon}(Q, \omega)$. This paper describes comparisons of experimental data with a theory of relaxation in complex correlated systems now generally referred to as the coupling model [13,14]. These comparisons show the Q and t dependences of $F_{relax}(Q, t)$ are in accord with the predictions of the coupling model. Parameters characterizing the relaxation process extracted from $F_s(Q, t)$ are found to have the physical meaning required by the coupling model.

2. The coupling model

The coupling model since its introduction in 1979 has repeatedly offered an accurate description of cooperative relaxation processes in dense packed correlated systems such as glass forming liquids [14]. It proposes the existence of a temperature insensitive crossover time, t_c, separating two time regimes in which the dynamics of relaxation differ. While the existence of t_c is suggested by theoretical considerations [13], its exact magnitude is not known a priori. Order of magnitude estimates of t_c obtained from comparing experimental data with the predictions of the coupling model locate it within the range $10^{-12} < t_c < 10^{-11}$ s for local segmental relaxation in polymers and translational and rotational motions in small molecular van der Waal liquids. An estimate roughly of 10^{-12} s has been suggested for ion motion in alkali borate glasses [15].

At short times, for $t < t_c$, the units relax independently, as if the intermolecular interaction had no effect, with a rate $W_0 \equiv 1/\tau_0$. However, for $t > t_c$, intermolecular interaction or constraints take hold, and on the average slow the independent relaxation rate. The result is that the effective relaxation rate obtained by averaging over all units has the time-dependent form $W(t) \propto W_0(t/t_c)^{-n}$, where n $(0 < n < 1)$ is the coupling parameter indicating the degree of intermolecular cooperativity. As far as the normalized correlation function, $C(t)$, for translational or rotational motion is concerned, the immediate consequence are

$$C(t) = \exp(-t/\tau_0) \quad \text{for } t < t_c; \tag{1}$$

$$C(t) = \exp - (t/\tau^*)^{1-n} \quad \text{for } t > t_c. \tag{2}$$

The important relation between τ^* and τ_0 given by

$$\tau^* = \left[t_c^{-n}\, \tau_0\right]^{1/(1-n)}. \tag{3}$$

is a consequence of the requirement that the two forms (1) and (2) of the correlation function should be continuous at the crossover time, t_c. In many occasions in the past we have written a similar relation $\tau^* = [(1-n)\omega_c^n \tau_0]^{1/(1-n)}$ where the reciprocal of ω_c is the time at which the relaxation rate defined by $-(1/C(t))\, dC(t)/dt$ are equal for the two correlation functions (Eqs. (1) and (2)). It can be easily shown that $t_c = (1-n)^{-1/n}\omega_c^{-1}$. Hence this relation and Eq. (3) are identical. The coupling parameter, n, through Eqs. (2) and (3) describes the effect that intermolecular interactions (or constraint dynamics) have in slowing the relaxation process.

The fractional exponential function given by Eq. (2) is identical to the relaxation function, $\exp[-(t/\tau)^\beta]$, first proposed by Kohlrausch [16] in 1847 to describe his electrical and mechanical relaxation data. Compilation of data taken over the past hundred and fifty years indicates that the Kohlrausch functions describe many relaxation processes in various families of materials rather well. Currently in the research community there are many efforts to explain the origin of the Kohlrausch function and meaning of the fractional exponent β. These efforts other than the coupling model include the mode–mode coupling theory of Götze and Sjögren [10,17], and the constraint theory of Phillips [18].

The three coupled relations given by Eqs. (1)–(3), were first proposed more than fourteen years ago and have remained unmodified [13,14]. They look deceptively simple but, in reality, when used together explain a host of important and often critical experimental fact concerning the viscoelastic response of amorphous polymers and small molecule glasses, and the diffusion of ions in glassy ionic conductors [14]. Most effective is the relation (3) between τ^* and τ_0, through which many previously puzzling properties have been explained (for a very recent review, see Ref. [14]). In these applications the experimental data had been obtained in the long time regime ($t \gg t_c$), which precludes direct observation of the crossover at t_c from exponential relaxation (1) to stretched exponential relaxation (2). Nevertheless, with the assumption of a temperature-insensitive t_c, the two coupled predictions (2) and (3) have been successful in explaining experimental data. Naturally, in view of this good agreement, it is desirable to directly verify the coupling model in its entirety (i.e., the existence of a temperature-independent t_c and the result in Eqs. (1)–(3)) either by rigorous theoretical proof or by performing experiments in time windows that span t_c. Recent attempts on the theoretical front based on the dynamics of chaotic Hamiltonians have produced encouraging results [13], although there is still a long way to go before the problem can be considered solved. On the other hand direct, experimental tests of the coupling model can be performed using QENS and MDS, which monitor the dynamics in the time window of $10^{-14} < t < 10^{-9}$ s, where the expected crossover of relaxation dynamics at t_c can be observed directly.

3. Quasielastic neutron scattering

The quasielastic neutron scattering measurements were made by Colmenero and co-workers [5,6] using the TOF spectrometer IN6 at the Institut Laue–Langevin, Grenoble, France. The incoherent scattering function, $S(Q, \omega)$, was obtained for various scattering wavevectors, Q, in the range $0.2 < Q < 2$ Å^{-1} and energy transfer, $\hbar\omega$, up to 5 meV at constant temperatures in the range $T_g - 8 < T < T_g + 100$ K. The poly(vinylchloride) (PVC) sample studied has a glass temperature $T_g = 358$ K and a number-averaged molecular weight $M_n = 4.55 \times 10^4$. The relaxation contribution, $S^{relax}(Q, \omega)$, to the scattering was isolated after removal of the harmonic vibrational contribution from the measured $S(Q, \omega)$, taking into account the instrument resolution. Fourier transform of $S^{relax}(Q, \omega)$ gives the normalized intermediate scattering function $I_0(Q, t) \equiv F_{relax}(Q, t)$. The results are reproduced in Fig. 1(a) for different temperatures at a constant Q value of 1.5 Å^{-1}. It can be seen that, independent of T and Q, all the intermediate scattering functions exhibit a break in curvature at a time of about 1.7 ps, signifying a crossover of $I_0(Q, t)$ from one regime at short times ($t < 1.7$ ps) to another at long times ($t > 1.7$ ps). This crossover

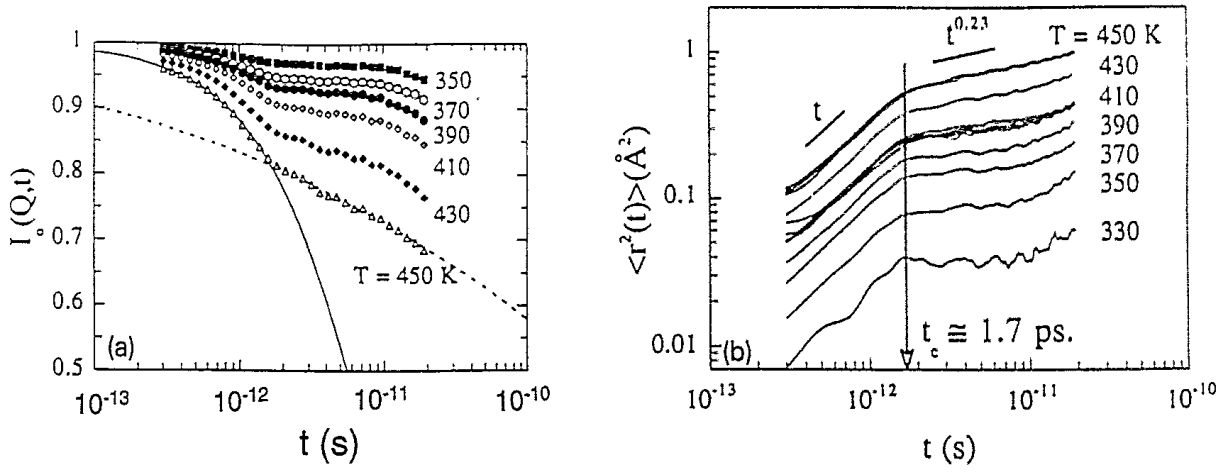

Fig. 1. (a) Normalized intermediate scattering function for PVC at $Q = 1.5$ Å^{-1} at different temperatures [5]. (b) Mean square displacement obtained from data in (a). For 450 K, data from different values of Q are plotted together [5].

between two different dynamic regimes is more clearly seen in the mean squared displacement of the scattering centers, $\langle r^2(t)\rangle$, which can be obtained from the $I_0(Q, t)$ data by solving the equation $I_0(Q, t) = \exp[-Q^2\langle r^2(t)\rangle/6]$. The values of $\langle r^2(t)\rangle$ so obtained [5,6] at different temperatures are plotted against time in Fig. 1(b), and the existence over a considerably large temperature range of a T-independent crossover time (approximately equal to 1.7 ps) is clear. In the short time regime of $t < 1.7$ ps, $\langle r^2(t)\rangle$ is proportional to t, while for $t > 1.7$ ps, $\langle r^2(t)\rangle \propto t^{1-n}$ with $n = 0.77$. This sublinear time dependence of $\langle r^2(t)\rangle$ was found previously using a longer time window of $10^{-11} < t < 10^{-8}$ s [19,20]. It has been shown to originate from the local segmental (alpha) relaxation of PVC, with a stretched exponential form, $\exp[-(t/\tau^*(Q, T))^{1-n}]$, for the intermediate scattering function.

To see if this crossover corresponds to the one proposed by the coupling model, the intermediate scattering function data in the short time regime was fitted by [5,6]

$$I_0(Q, t) = \exp - \big(t/\tau_0(Q, T)\big) \quad \text{for } t < 1.7 \text{ ps} \tag{4}$$

and the data in the long time regime by the stretched exponential (see Fig. 1(a))

$$I_0(Q, t) = \exp - \big[t/\tau^*(Q, T)\big]^{1-n} \quad \text{for } t > 1.7 \text{ ps} \tag{5}$$

with the exponent $1 - n$ taken to be that obtained from $\langle r^2(t)\rangle \propto t^{1-n}$ (i.e., $1 - n = 0.23$ for $T = 430$ and 450 K (see Fig. 1(b))). While fits to Eq. (4) (solid curve in Fig. 1(a)) in the short time regime have been carried out successfully in the entire temperature range, fits to Eq. (5) in the long time regime can be carried out with confidence at only the two highest temperatures, 430 and 450 K, where the $I_0(Q, T)$ data decrease significantly with time, before being cut off by the long time edge of the time window. These fits, shown as dashed curves in Fig. 1(a), describe well the experimental $I_0(Q, T)$ at $T = 430$ and 450 K.

From these fits of the experimental data in the two separate time regimes using Eqs. (4) and (5), τ_0 and τ^* were obtained as a function of Q and T. For τ_0 it was found that

$$\tau_0(Q, T) \propto Q^{-2} \exp\big[(5.8 \text{ kcal/mol})/RT\big]. \tag{6}$$

The Q^{-2} dependence indicates simple diffusion of the scattering centers, consistent with independent relaxation of local segments without the intermolecular interaction expected for $t < t_c$. The Arrhenius temperature dependence is valid over a temperature range and has an activation enthalpy of about 6 kcal/mol. This enthalpy is comparable to the conformational energy barrier of a PVC chain deduced before from different measurements [21]. Such a temperature dependence provides additional support for the coupling model interpretation of the short time ($t < t_c$) dynamics. On the other hand, for τ^*, combining the current TOF neutron scattering data with the previously published neutron backscattering data, we find $\tau^* \propto Q^{-9}$, similar to earlier results

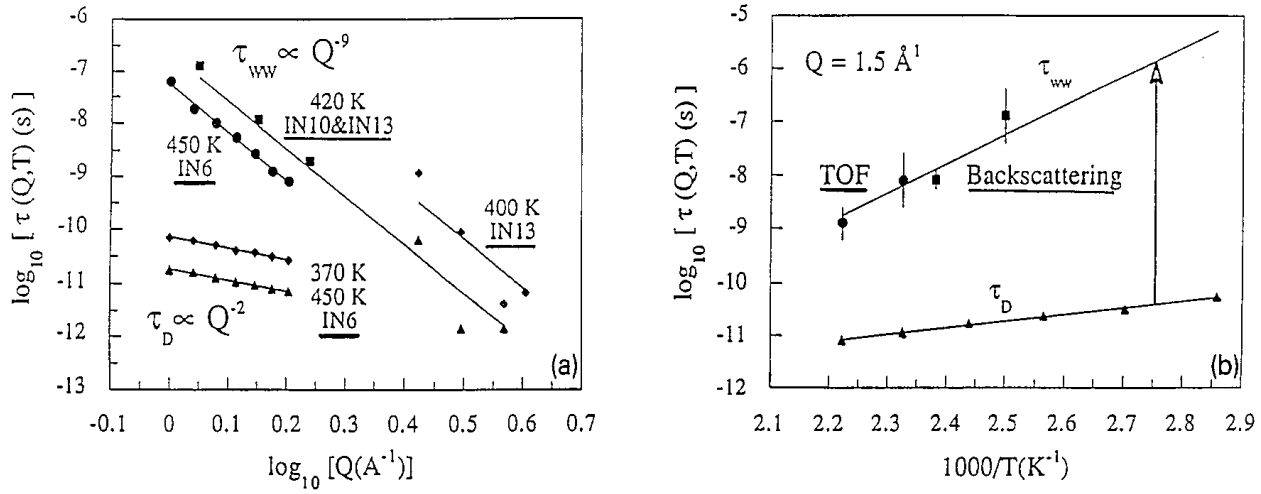

Fig. 2. (a) Q-dependences of τ_0 and τ^* [5]. (b) T-dependences of τ_0 and τ^* [5].

[19,20] based on backscattering data alone. Substituting $\tau_0(Q, T)$ given by Eq. (6) into Eq. (3), recalling the fact that t_c is independent of Q and T and $n = 0.77$, the coupling model predicts

$$\tau^*(Q, T) \propto Q^{-2/(1-0.77)} \times \exp\{25\ (\text{kcal/mol})/RT\}. \qquad (7)$$

These predicted temperature and Q dependencies of τ_0 and τ^* are summarized and illustrated respectively in Figs. 2(a) and (b). The predictions are in good agreement with the experimental data. Similar results have been obtained for other polymers including poly(vinylmethylether), polybutadiene and polyisoprene [22]. Thus, we conclude that neutron scattering data directly corroborate the coupling model.

Questions can be raised on the plausibility of the observation of diffusive motion (consistent with the Q^{-2} dependence of τ_0 in Eq. (6)) in the short time regime of $3 \times 10^{-13} < t < t_c$. In fact, the existence of a multitude of high frequency vibrational (bond bending and stretching) modes provides the fast variables (i.e., heat bath) that enable 'diffusion' of the hydrogen as seen by the neutrons. In the next section we discuss molecular dynamics simulation of small molecule liquids and polymers. In these simulations [7–9], the same crossover phenomenon seen by incoherent neutron scattering are obtained, with similar t_c for both $F_s(q, t)$ and the reorientational time correlation function, $M_k(t) = \langle P_k[\cos\theta(t)]\rangle$, where $P_k(x)$ is the Legendre polynomial of order k, and $\theta(t)$ is the reorientation angle of a vector at time, t. For reorientational motion, the rotational diffusion relaxation time does not have any Q-dependence, and it is obvious that rotational diffusion can occur on timescales of the order of a picosecond.

4. Molecular dynamics simulations

In recent years improvement in the technique has made molecular dynamics simulation (MDS) a powerful tool to investigate the dynamics of molten salts [7], glass-forming small molecule liquids [8] and polymers [9]. Realistic potentials have been used to represent the interactions between the molecular units, making the results of computer experiments as quantitatively accurate as actual experiments. In addition, information extracted from MDS are often richer than that from real experiments. Thus, these MDS data provide additional tests of the theoretical basis of the coupling model. In this section we analyze one set of MDS data [9] and show that the results confirm the coupling model's description of the dynamics.

Roe [9] has performed MDS of polyethylene (PE). The intermolecular interactions are of the short range van der Waals kind, represented by Lennard–Jones potentials. $F_s(Q, T) = \langle \exp\{-iq \cdot [r_i(t) - r_i(0)]\}\rangle$, where $r_i(t)$ is the position of the ith segment at time, t, has been evaluated for different temperatures and several values of the wavevector, Q. Results for $Q = 1.38\ \text{Å}^{-1}$ are shown in Ref. [9]. At temperatures < 108 K there is an initial decay of $F_s(Q, T)$ which can be ascribed to harmonic phonons, with no additional relaxation process observed in the time window. The assignment of the initial decay to harmonic phonons is consistent with the plateau value, $F_s(Q, T \rightarrow \text{large})$, being well described by the Debye–Waller factor, $\exp(-WQ^2T)$, where W is a constant independent of Q and T [23]. A semilog plot of the Debye–Waller factor obtained from the low temperature $F_s(Q, T)$ data yields a straight line which can be used to extrapolate the phonon contribution to higher temperatures. This extrapolation clearly indicates that the contribution of phonons to $F_s(Q, T)$ has to be taken into consideration at all temperatures. At temperatures $\geqslant 132$ K, additional relaxation processes appear in the time window of Fig. 3, making it difficult to isolate the individual components. We can account for the harmonic phonon contribution to $F_s(Q, T)$ at higher temperatures by Fourier transformation of the $F_s(Q, T)$ data at low temperatures (say $T < 108$ K), where only the harmonic phonons contribute, followed by scaling of the resultant dynamic structure factor, $S(Q, \omega)$, by the Bose factor and the Debye–Waller factors [23]. The inverse Fourier transform of the scaled $S(Q, \omega)$ yields $F_s^{\text{ph}}(Q, t)$, the density–density correlation function from phonons at higher temperatures. Assuming that scattering by harmonic phonons and relaxation are statistically independent processes, we write the intermediate scattering function as a product $F_s(Q, t) = F^{\text{phonon}}(Q, t)F^{\text{relax}}(Q, t)$. Eq. (3) can be solved for $F^{\text{relax}}(Q, t)$ at any T. The results can be compared with the predictions of the coupling model in a

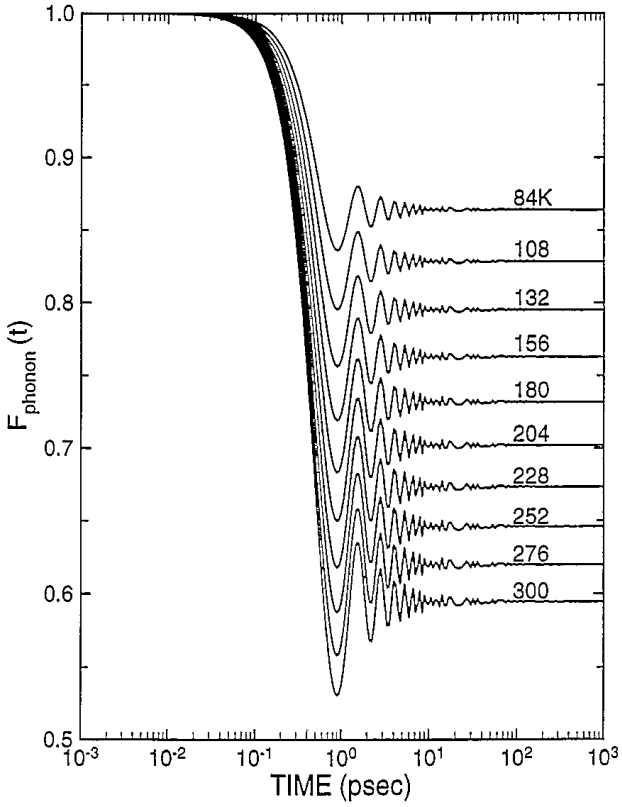

Fig. 3. $F_{phonon}(Q, t; T)$ plotted against t for $q = 1.38$ Å^{-1} at different temperatures.

similar manner as done previously by Colmenero and co-workers [5,6] using their QENS data.

In this paper we model the phonons contributing to $F_{phonon}(Q, t; T)$ at temperature, T, by a Debye spectrum with density of normal modes, $g_D(\omega)$, represented in the form of $g_D(\omega) = (3/2\pi^2)(\omega^2/c^2) \equiv K\omega^2$ for $\omega < \omega_D$ and $g_D(\omega) = 0$ for $\omega > \omega_D$. Although the Debye spectrum is only a gross approximation, we use it because of simplicity and to avoid the possibility of biasing the final results. Using a well known expression [24], $F_{phonon}(Q, t; T)$ is calculated for a Debye spectrum of phonons $g_D(\omega)$ according to the formula $F_{phonon}(Q, t; T) = \exp(-Q^2 W(t, T))$ at T, where

$$W(t, T) = KT^2 \int_0^{\omega_D} g_D(\omega)[1-\cos(\omega t)]\,\omega^{-1} \times [2/(\exp(\hbar\omega/kT) - 1) + 1]\,\mathrm{d}\omega. \quad (8)$$

The parameters K and ω_D are adjusted to fit the experimental $F_s(Q, t; T)$ obtained at the lowest temperatures, where $F_{relax}(Q, t; T) = 1$ throughout the experimental range of time. For the data of Roe [9] at $Q = 1.38$ Å^{-1}, we find $\omega_D = 5 \times 10^{12}$ rad/s and $K = 6.83 \times 10^{-30}$. The $F_{phonon}(Q, t; T)$ at all temperatures for which Roe has made his simulations are displayed in Fig. 3. We can now assess the coupling model by examining whether the experimental $F_s(Q, t; T)$ can be represented at each temperature by

$$F_s(Q, t; T) = F_{phonon}(Q, t; T) \times \begin{cases} \exp - (t/\tau_0(T)) & \text{for } t < t_c \\ \exp - (t/\tau^*(T))^{1-n} & \text{for } t > t_c \end{cases}, \quad (9)$$

for a temperature-independent t_c such that the continuity condition, $\exp - (t/\tau_0(T)) = \exp - (t/\tau^*(T))^{1-n}$, is satisfied always at $t = t_c$. We start by first choosing a t_c and then for each temperature find two independent parameters, τ_0 and n (the third parameter τ^* is automatically fixed by Eq. (3)), such that the products on the right hand side of Eq. (9) give a good fit to the experimental $F_s(Q, t; T)$. In carrying out this, we find that for good fits at all temperatures can only be obtained for values of t_c limited to a narrow range around 2 ps.

The results of the best fits for $t_c = 2$ ps are shown in Fig. 4. The $F_{relax}(Q, t; T)$ used to obtain these fits are displayed in Fig. 5. At each temperature, $F_{relax}(Q, t; T)$ is comprised of two pieces: $\exp - (t/\tau_0(T))$ for $t < t_c$ and $\exp - (t/\tau^*(T))^{1-n(T)}$ for $t > t_c$. The relaxation times, τ_0 and τ^*, and the

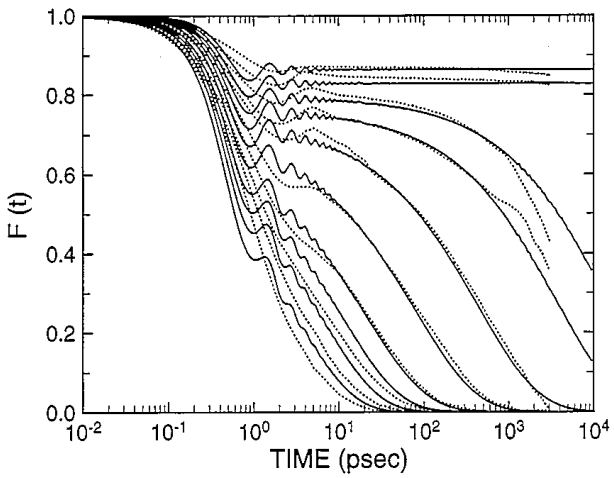

Fig. 4. Theoretical fits (solid curves) to experimental data (dotted curves) $F_s(Q, t; T)$ of polyethylene.

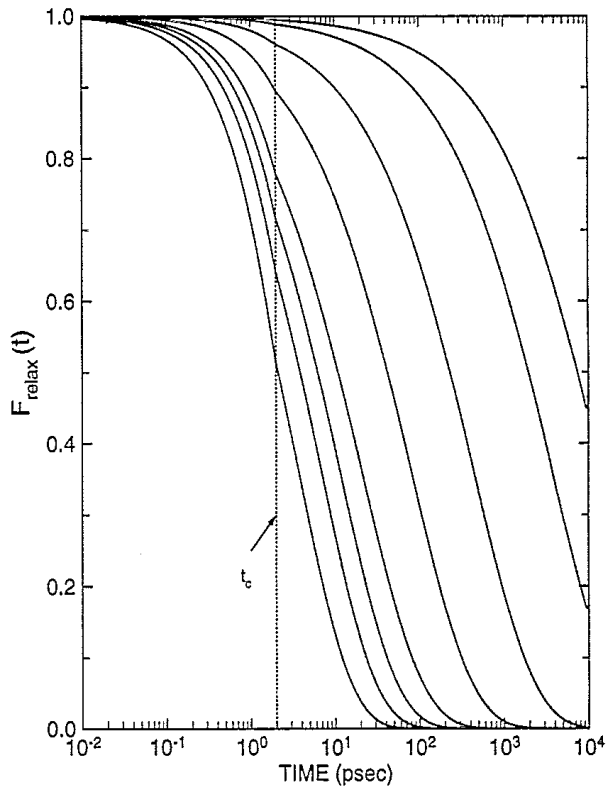

Fig. 5. $F_{relax}(Q, t;T)$ at different temperatures.

coupling parameter, n, are plotted as a function of temperature in Fig. 6 and Fig. 7, respectively. The temperature dependence of τ_0 is approximately Arrhenius with an activation enthalpy of about $E_a = 2.4$ kcal/mol. It is apparent that the temperature dependence of τ_0 becomes milder at high temperatures ≥ 252 K, which makes the overall activation energy to appear smaller. Excluding the three highest temperatures, the activation enthalpy is close to 3 kcal/mol.

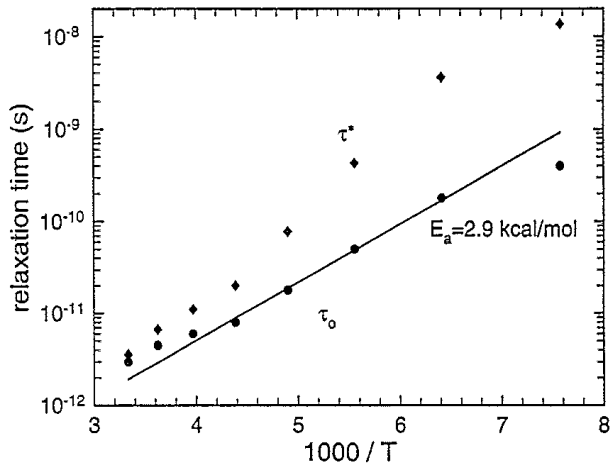

Fig 6. Arrhenius plot of τ_0 and τ^* of polyethylene.

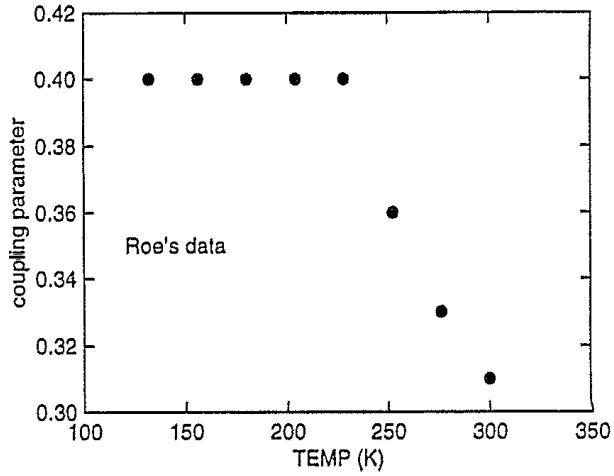

Fig. 7. The coupling parameter, n, as a function of temperature.

The coupling parameter has the value of 0.40 and exhibits a decrease at high temperatures. This decrease of n at high temperatures may be correlated with the corresponding milder temperature dependence of τ_0 seen there. The value for E_a is roughly what is expected for the activation energy of the conformational energy barrier for a single polyethylene chain. As modelled by Roe, this is about 3 kcal/mol [9]. This is a striking agreement for the microscopic activation energy which governs local segmental motion of a single chain. The stretch exponent, $\beta \equiv 1 - n$, determined for polyethylene is close to that expected from the empirical correlation between β and the steepness of the polymer's cooperative plot [25]. The coupling parameter $n = 0.40$ for polyethylene is smaller than that of all other polymers with bulkier monomer structure. The much larger coupling parameter ($n = 0.77$) found for polyvinylchloride (PVC) from QENS as well as dielectric and mechanical measurements, arises from its larger intermolecular interaction due to the polar nature of the PVC backbone. The disparity of the values of n in PVC and PE is directly responsible for the different appearance of the $F_{relax}(Q, t; T)$s obtained for these two polymers (see Fig. 1(a) and Fig. 5). In PVC we see clearly a break in the $F_{relax}(Q, t; T)$ at the crossover time, t_c. For PE, the break at the crossover is less obvious (Fig. 5) due to the smaller n. Nevertheless, in PE the initial exp $-(t/\tau_0(T))$ decay for $t < t_c$ is necessary to explain the

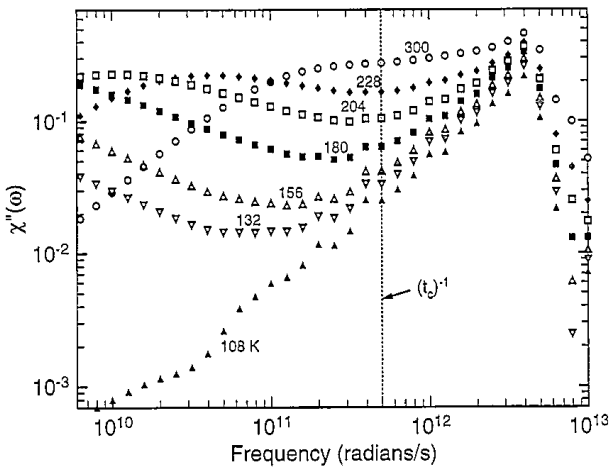

Fig. 8. Calculated $\chi''(\omega)$ at different temperatures.

departure of $F_s(Q, t; T)$ from the phonon contribution $F_{\text{phonon}}(Q, t; T)$ at short times.

Finally we calculate from $F_s(Q, t; T)$ by temporal Fourier transform the functions $S(Q, \omega; T)$ and $\chi''(Q, \omega; T)$. The results for $\chi''(\omega)$ are shown in Fig. 8. The resemblance of these results to those obtained by depolarized light scattering on $[Ca(NO_3)_2]_{0.4}[KNO_3]_{0.6}$ and salol [26] merits futher discussion, but is beyond the scope of the present paper.

5. Conclusion

Quasielastic neutron scattering and molecular dynamics simulation data provide critical tests of the basic premise of the coupling model. From the analyses of the data given above for two polymers and other glass-forming materials (including the molten salt $[Ca(NO_3)_2]_{0.4}[K(NO)_3]_{0.6}$ [7] and ortho-terphenyl [8]) not discussed here, we conclude that these experimental data are in agreement with the fundamental laws of relaxation (specifically, Eqs. (1)–(3) with a temperature-independent t_c) for interacting systems as postulated by the model. In addition to this simplicity, the model has the virtue of being applicable to different materials and phenomena. By means of Eq. (3), many observed anomalies can be explained. Some examples that support these claims can be found in a recent review [14].

K.L.N. is supported in part by ONR Contract N0001494WX23010. The authors thank A. Arbe, Juan Colmenero, Laurent Lewis and R.J. Roe for making their published data available and permission to reproduce some of these published data.

References

[1] W. Knaak, F. Mezei and B. Farago, Europhys. Lett. 7 (1988) 529.
[2] B. Frick, B. Farago and D. Richter, Phys. Rev. Lett. 64 (1990) 2921.
[3] W. Petry, E. Bartsch, F. Fujara, M. Kiebel, H. Sillescu and B. Farago, Z. Phys. B83 (1991) 175.
[4] M. Kiebel, E. Bartsch, O. Debus, F. Fujara, W. Petry and H. Sillescu, Phys. Rev. B45 (1992) 10301.
[5] J. Colmenero, A. Arbe and A. Alegría, Phys. Rev. Lett. 71 (1993) 2603.
[6] J. Colmenero, Physica A201 (1993) 38.
[7] G.F. Signorini, J.L. Barrat and M.L. Klein, J. Chem. Phys. 92 (1990) 1294.
[8] L.J. Lewis and G. Wahnström, J. Non-Cryst. Solids 172–174 (1994) 69.
[9] R.J. Roe, J. Chem. Phys. 100 (1994), 1610; J. Non-Cryst. Solids 172–174 (1994) 77.
[10] W. Götze and L. Sjögren, Rep. Progr. Phys. 55 (1992) 241.
[11] X.C. Zeng, D. Kivelson and G. Tajus, J. Non-Cryst. Solids 172–174 (1994) 61.
[12] P.K. Dixon, N. Menon and S.R. Nagel, Phys. Rev. E50 (1994) 1717;
H.Z. Cummins and G. Li, Phys. Rev. E50 (1994) 1720.
[13] K.L. Ngai, Comment Solid State Phys. 9 (1979) 127; K.L. Ngai and R.W. Rendell, J. Non-Cryst. Solids 131–133 (1991) 233; K.L. Ngai, S.L. Peng and K.Y. Tsang, Physica, A191 (1992) 523; K.Y. Tsang and K.L. Ngai, to be published.
[14] K.L. Ngai, in: Disorder Effects in Relaxation Processes, ed. A. Blumen and R. Richert (Springer, Heidelberg, 1994) p. 89.
[15] K.L. Ngai and H. Jain, Solid State Ionics 18&19 (1986) 362.
[16] R. Kohlrausch, Ann. Phys. (Leipzig) 12 (1847);
G. Williams and D.C. Watts, Trans. Faraday Soc.66 (1970) 80.
[17] W. Götze and L. Sjögren, J. Non-Cryst. Solids 172–174 (1994) 16.
[18] J.C. Phillips, J. Non-Cryst. Solids 172–174 (1994) 98.
[19] J. Colmenero, A. Arbe, A. Alegría and B. Frick, Phys. Rev. Lett. 69 (1992), 478.
[20] K.L. Ngai, J. Colmenero, A. Arbe and Alegría, Macromolecules 25 (1992), 6727.
[21] K.L. Ngai and A.F. Yee, J. Polymer Sci. B: 29 (1991) 1493.
[22] J. Colmenero, private communication (1994).
[23] N.W. Ashcroft and N.D. Mermin, Solid State Physics (Holt, Rinehart and Winston, New York, 1976) appendix N.
[24] We thank Prof. Wolfgang Dieterich for an illuminating discussion.
[25] K.L. Ngai and C.M. Roland, Macromolecules 26 (1993) 6824.
[26] H.Z. Cummins, W.M. Du, M. Fuchs, W. Götze, A. Latz, G. Li and N.J. Tao, Physica A201 (1993) 23.